

Supporting Information

A Naphthalimide-Quinoline based probe for selective, fluorescence ratiometric sensing of trivalent ions

Shyamaprosad Goswami* , Krishnendu Aich, Avijit Kumar Das, Abhishek Manna and Sangita Das

Department of Chemistry, Bengal Engineering and Science University, Shibpur, Howrah 711103, West Bengal, India E-mail: spgoswamical@yahoo.com; Fax: +91-3326682916.

CONTENTS

- 1. General procedure for drawing Job plot by fluorescence method.....**
- 2. Association constants and fluorescence titration curve of Sensor with M^{3+} ...**
- 3. Determination of detection limit.....**
- 4. Metal ion selectivity profile of the sensor.....**
- 5. 1H NMR (S5) and Mass spectra (S6) of receptor**
- 6. Fluorescence titration spectra of receptor with different guest cations**
- 7. UV-vis titration spectra of receptor with Fe^{3+} , Al^{3+} and Cr^{3+} **
- 8. X-ray Crystallographic data.....**

1. General procedure for drawing Job plot by fluorescence method:

Stock solution of same concentration of sensor and M^{3+} (where $M = Fe^{3+}$, Al^{3+} and Cr^{3+}) were prepared in the order of $20\mu M$ in $[CH_3CN/H_2O, 40/60, v/v]$ (at $25\text{ }^\circ C$) at pH 7.4 in HEPES buffer. The emission spectrum in each case with different *host-guest* ratio but equal in volume was recorded. Job plots were drawn by plotting $\Delta I \cdot X_{host}$ vs X_{host} (ΔI = change of intensity of the emission spectrum at 390 nm during titration and X_{host} is the mole fraction of the host in each case, respectively).

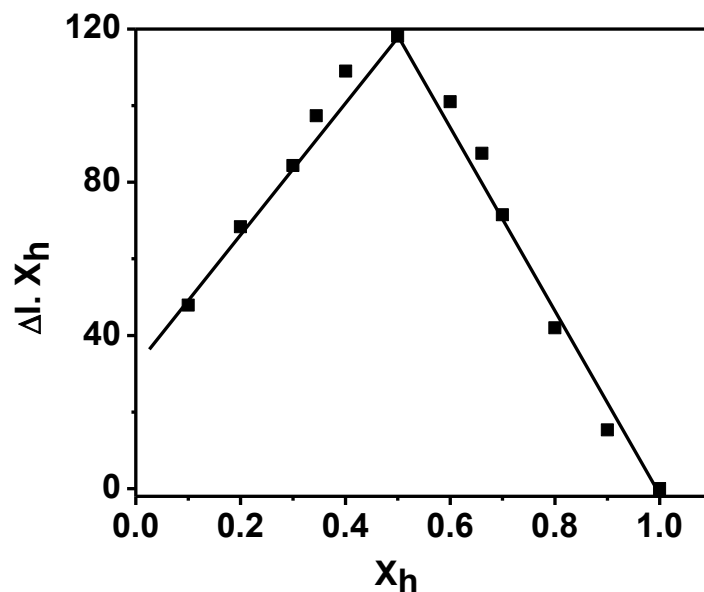


Figure S1: Job's plot diagram of receptor for Fe^{3+} ion (where X_h is the mole fraction of the host and ΔI indicates the change of emission intensity at 390 nm)

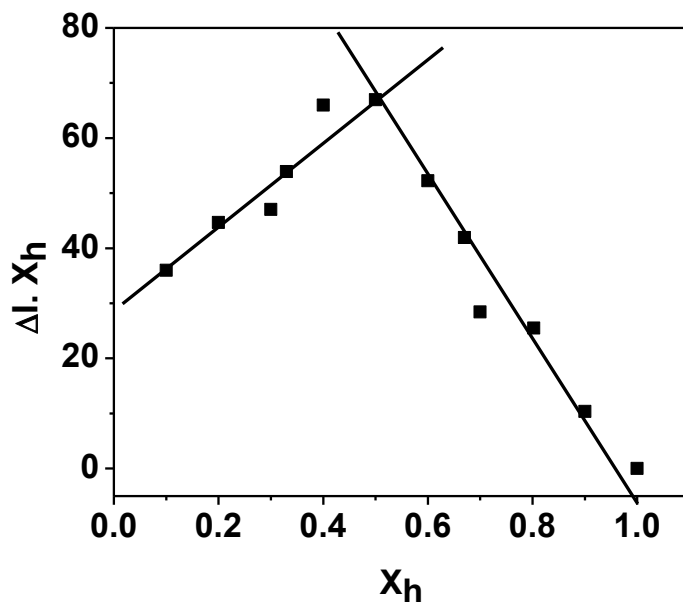


Figure S2: Job's plot diagram of receptor for Al^{3+} ion (where X_h is the mole fraction of the host and ΔI indicates the change of emission intensity at 390 nm)

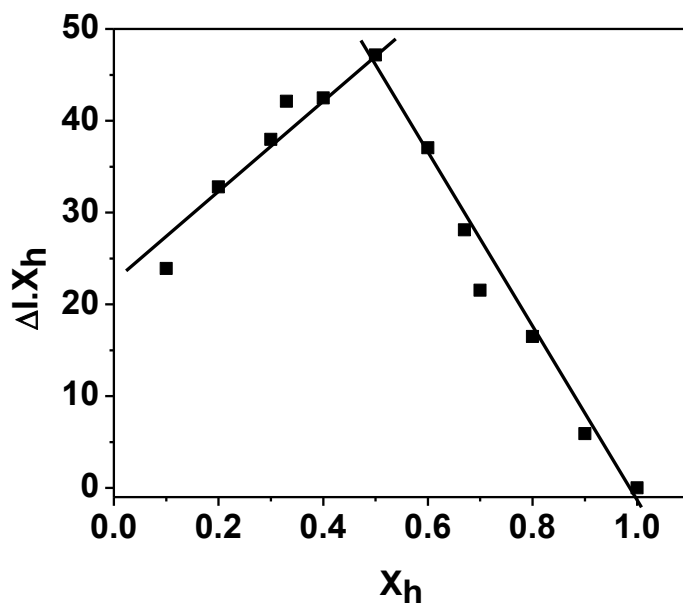


Figure S3: Job's plot diagram of receptor for Cr^{3+} ion (where X_h is the mole fraction of the host and ΔI indicates the change of emission intensity at 390 nm)

2. Association constant determination:

The binding constant value of M^{3+} (where $\text{M} = \text{Fe}^{3+}$, Al^{3+} and Cr^{3+}) with sensor has been determined from the emission intensity data following the modified Benesi-Hildebrand equation¹, $1/\Delta I = 1/\Delta I_{\text{max}} + (1/K[\text{C}]) (1/\Delta I_{\text{max}})$. Here $\Delta I = (I - I_{\text{min}})$ and $\Delta I_{\text{max}} = (I_{\text{max}} - I_{\text{min}})$, where I_{min} , I , and I_{max} are the emission intensities of sensor considered in the absence of M^{3+} , at an intermediate M^{3+} concentration, and at a concentration of complete saturation where K is the binding constant and $[\text{C}]$ is the M^{3+} concentration respectively. From the plot of $1/(I - I_{\text{min}})$ against $[\text{C}]^{-1}$ for sensor, the value of K has been determined from the ratio of intercept and slope of Benesi-Hildebrand plot. As the plot of $1/(I - I_{\text{min}})$ vs $1/[\text{C}]$ gives a straight line, indicates the 1:1 complexation of the sensor with M^{3+} . The association constant (K_a) as determined by fluorescence titration method for sensor with Fe^{3+} , Al^{3+} and Cr^{3+} are found to be $1.0852 \times 10^4 \text{ M}^{-1}$, $8.770 \times 10^3 \text{ M}^{-1}$ and $5.676 \times 10^3 \text{ M}^{-1}$ respectively (error $\pm 10\%$).

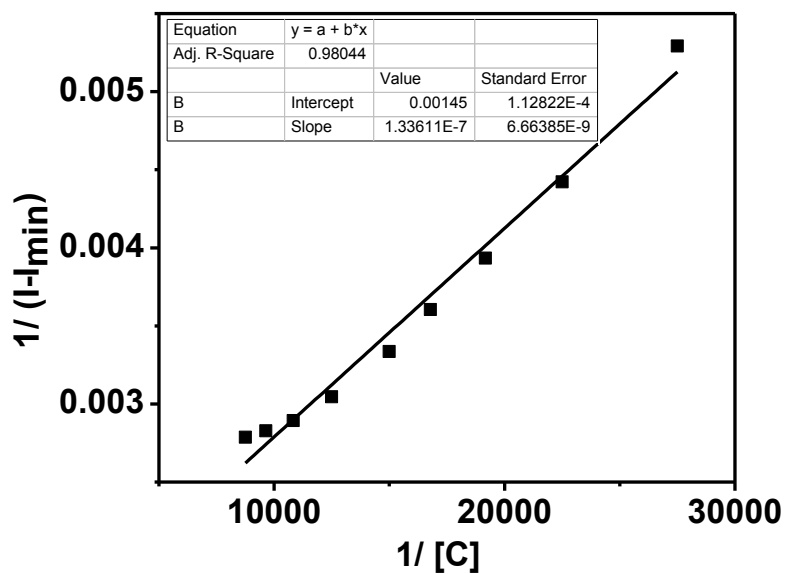


Figure S4: Benesi-Hildebrand plot from fluorescence titration data of receptor (20 μM) with Fe^{3+} .

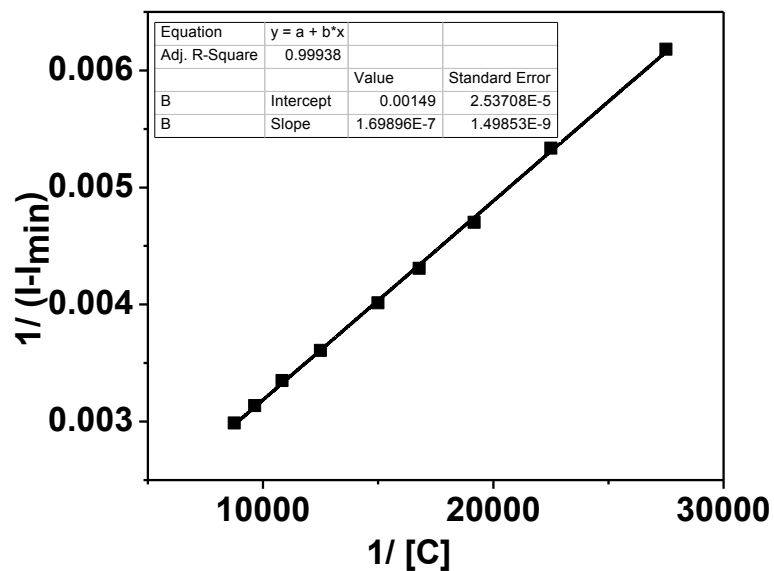


Figure S5: Benesi-Hildebrand plot from fluorescence titration data of receptor (20 μM) with Al^{3+} .

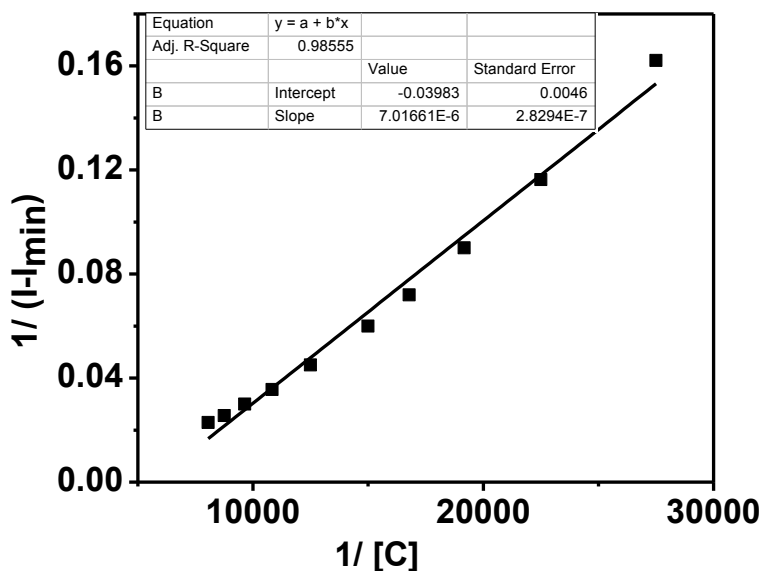


Figure S6: Benesi-Hildebrand plot from fluorescence titration data of receptor (20 μM) with Cr^{3+} .

3. Determination of detection limit:

The detection limit (DL) of NAQ for Fe^{3+} , Al^{3+} and Cr^{3+} were determined from the following equation:

$$\text{DL} = K * \text{Sb1}/\text{S}$$

Where $K = 2$ or 3 (we take 3 in this case); Sb1 is the standard deviation of the blank solution; S is the slope of the calibration curve.

For Fe^{3+} :

From the graph we get slope = 16700.99, and Sb1 value is 0.115058

Thus using the formula we get the Detection Limit = 20 μM i.e. NAQ can detect Fe^{3+} in this minimum concentration.

For Al^{3+} :

From the graph we get slope = 7.53E+03, and Sb1 value is 0.059735

Thus using the formula we get the Detection Limit = 23 μM i.e. NAQ can detect Al^{3+} in this minimum concentration.

For Cr^{3+} :

From the graph we get slope = 2662.453, and Sb1 value is 0.022587

Thus using the formula we get the Detection Limit = 25 μM i.e. NAQ can detect Cr^{3+} in this minimum concentration.

4. Metal ion selectivity profile of the sensor :

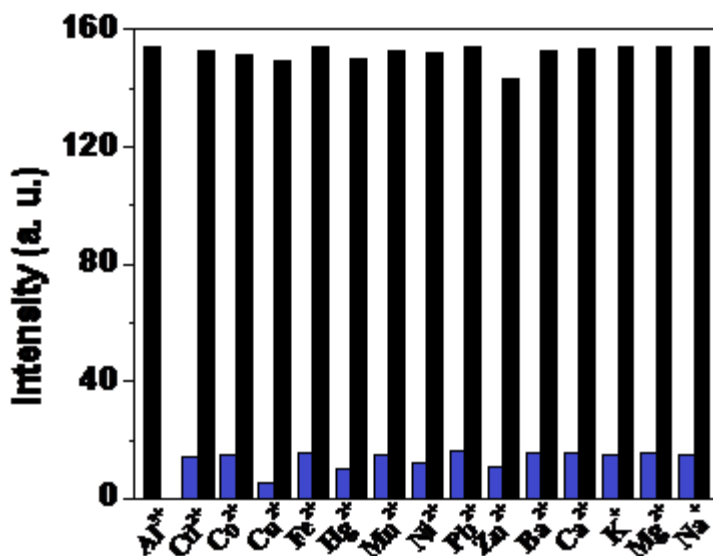


Figure S7: Metal ion selectivity profile of the receptor (20 μM): (black bars) change of emission intensity of receptor + 10 equiv M^{n+} ; (blue bars) change of emission intensity of receptor + 10 equiv M^{n+} , followed by 3 equiv Al^{3+} at 484 nm

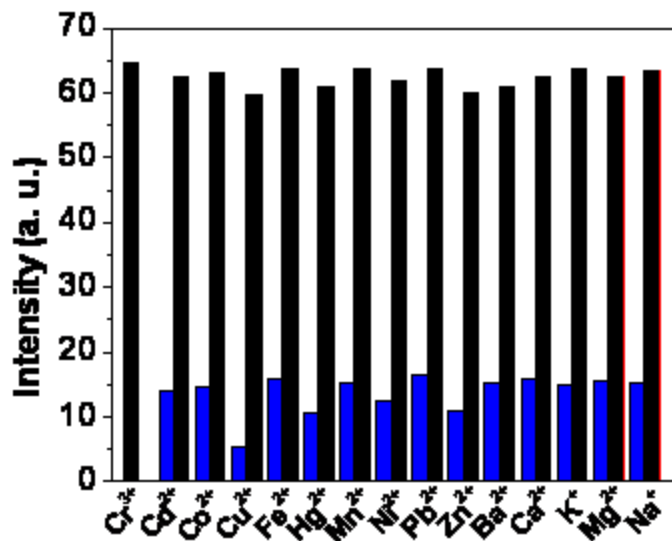
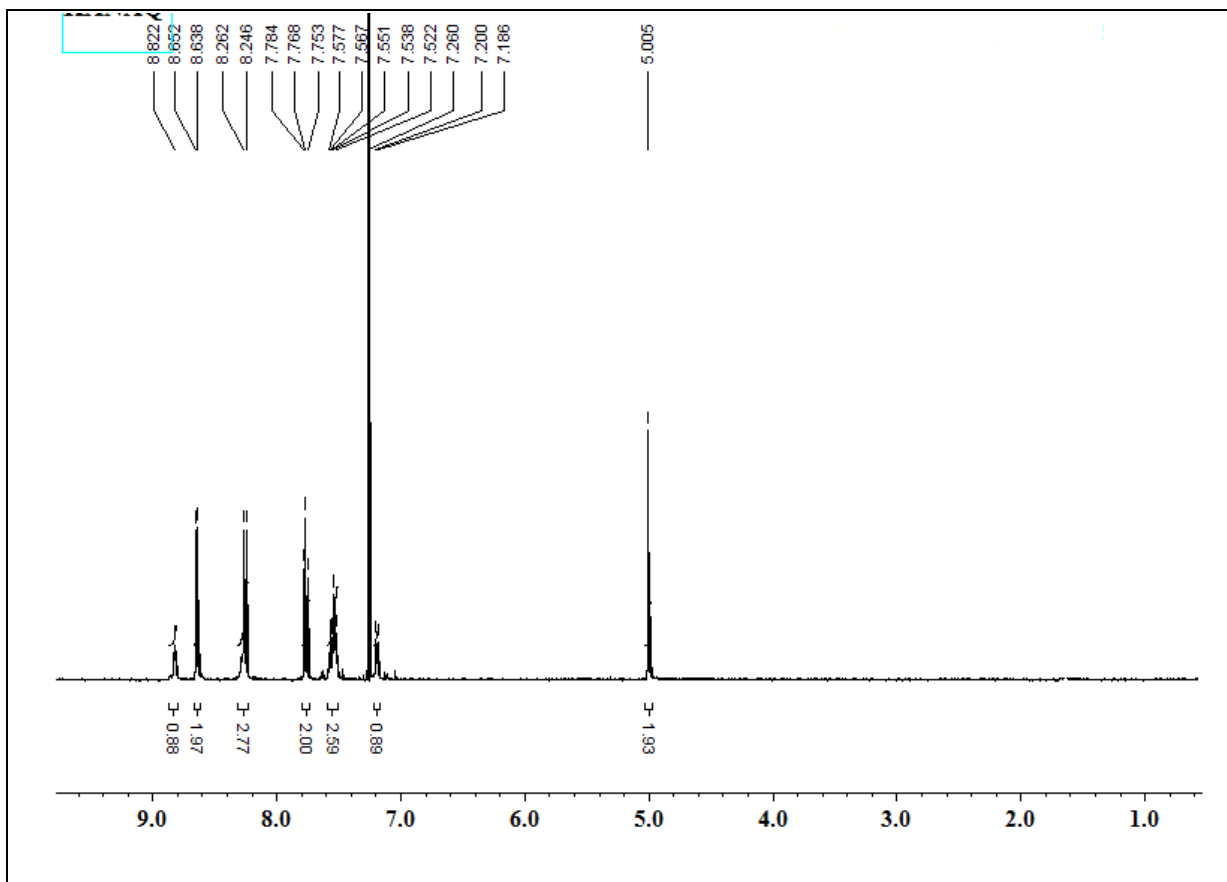
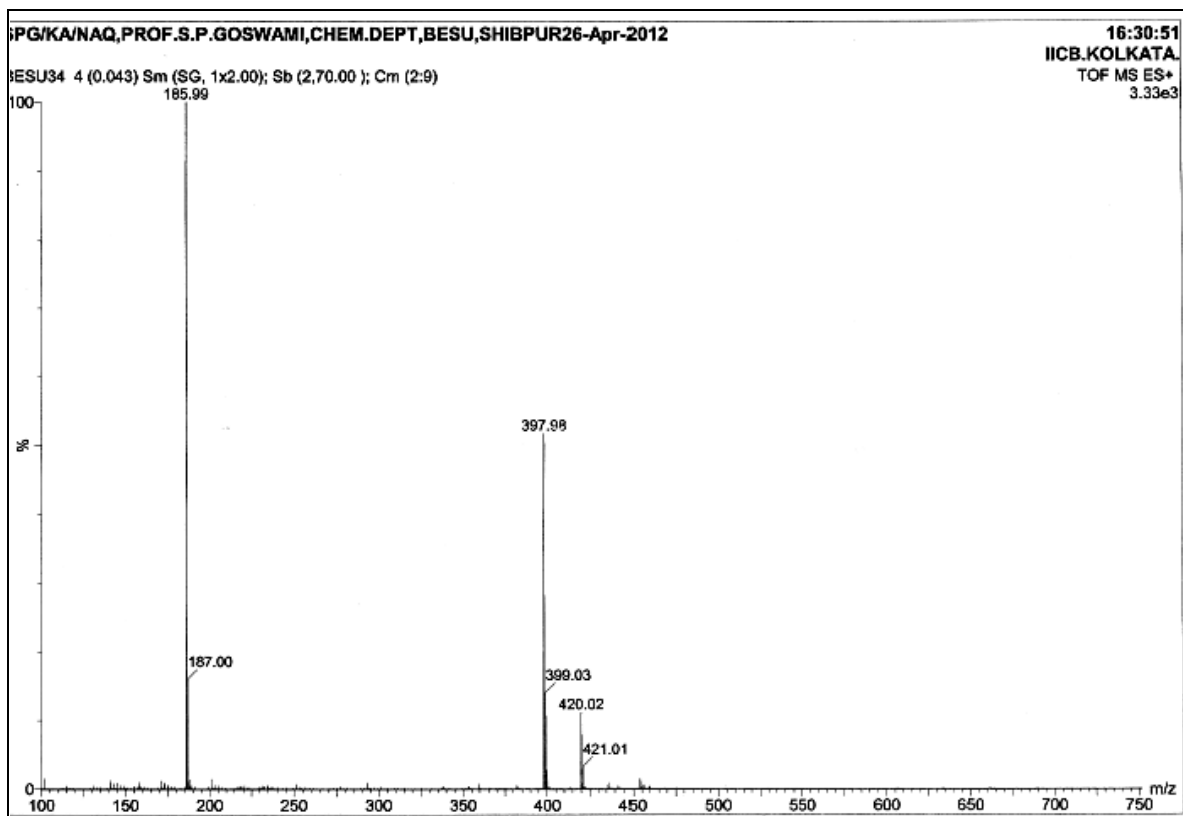


Figure S8: Metal ion selectivity profile of the receptor (20 μM): (black bars) change of emission intensity of receptor + 10 equiv M^{n+} ; (blue bars) change of emission intensity of receptor + 10 equiv M^{n+} , followed by 3 equiv Cr^{3+} at 484 nm

5.

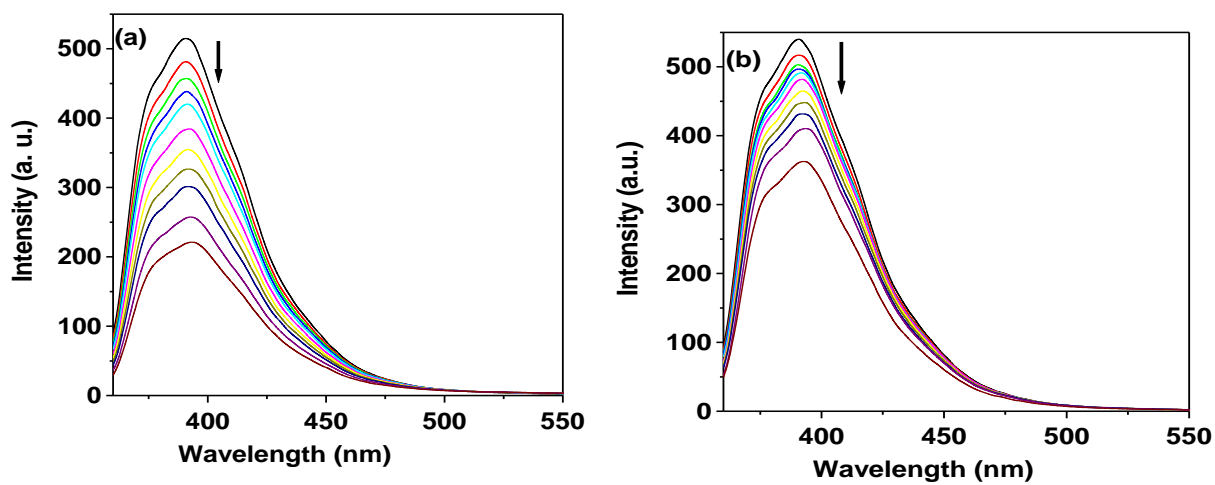


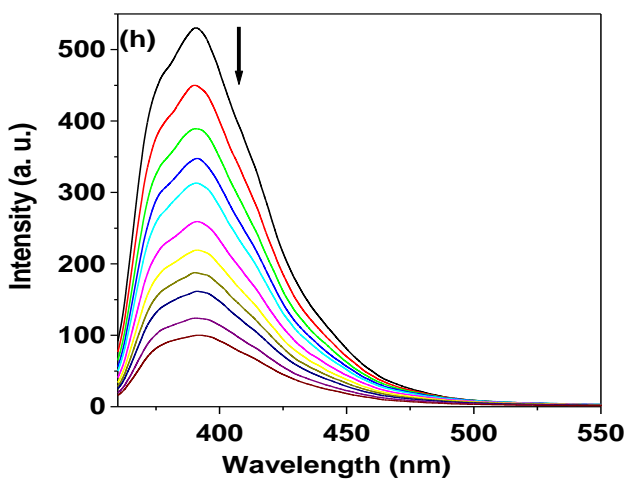
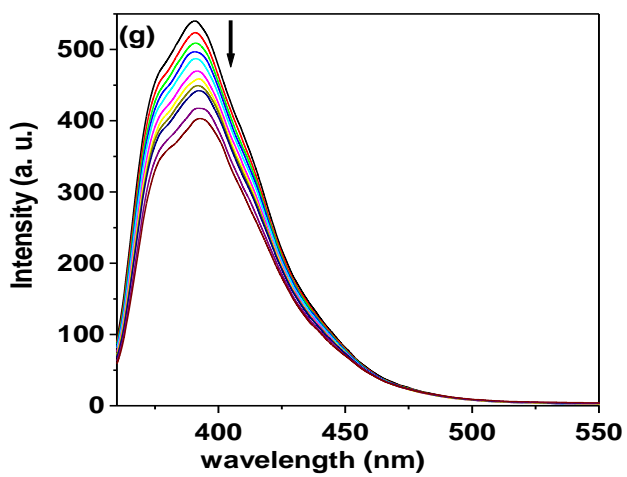
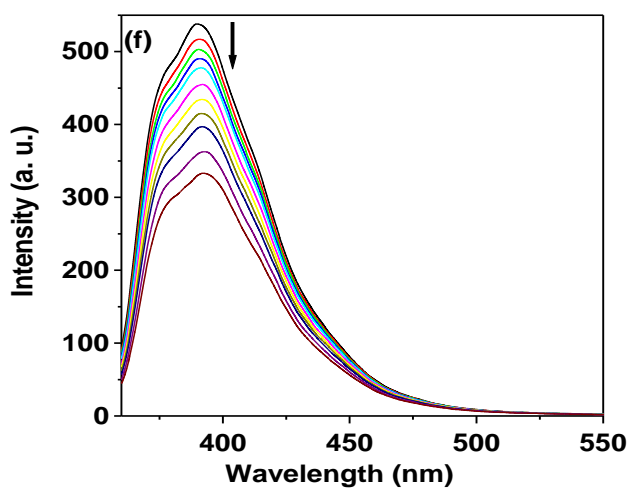
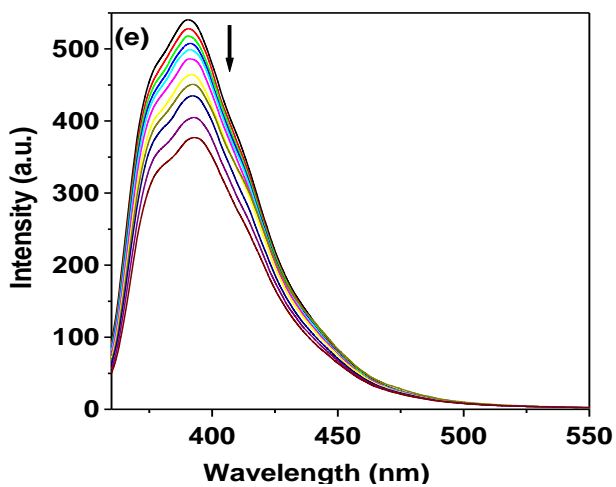
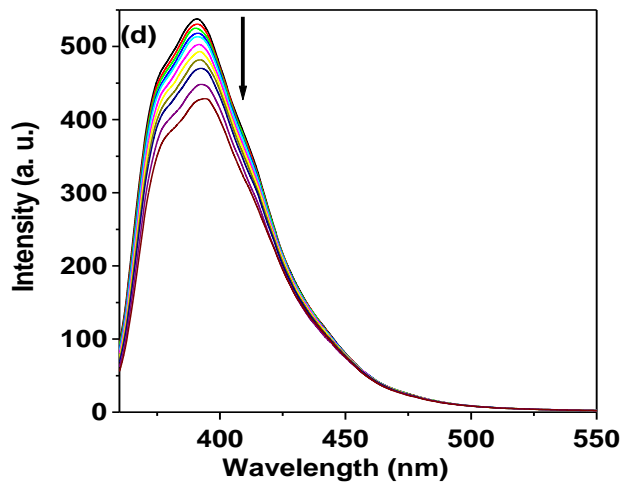
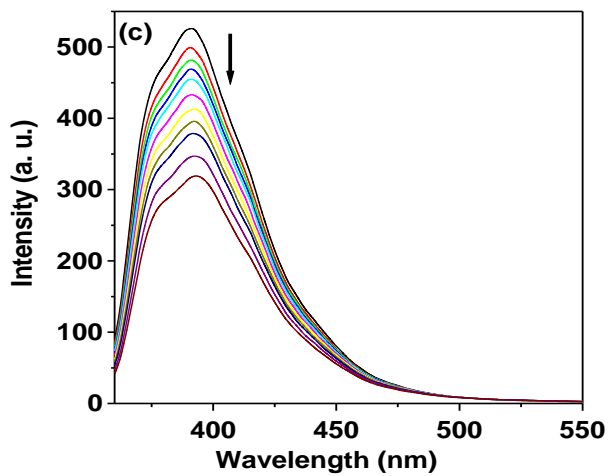
S9: ¹H NMR spectrum of NAQ



S10: Mass spectrum of NAQ.

6. Fluorescence titration spectra of receptor with different guest cations:





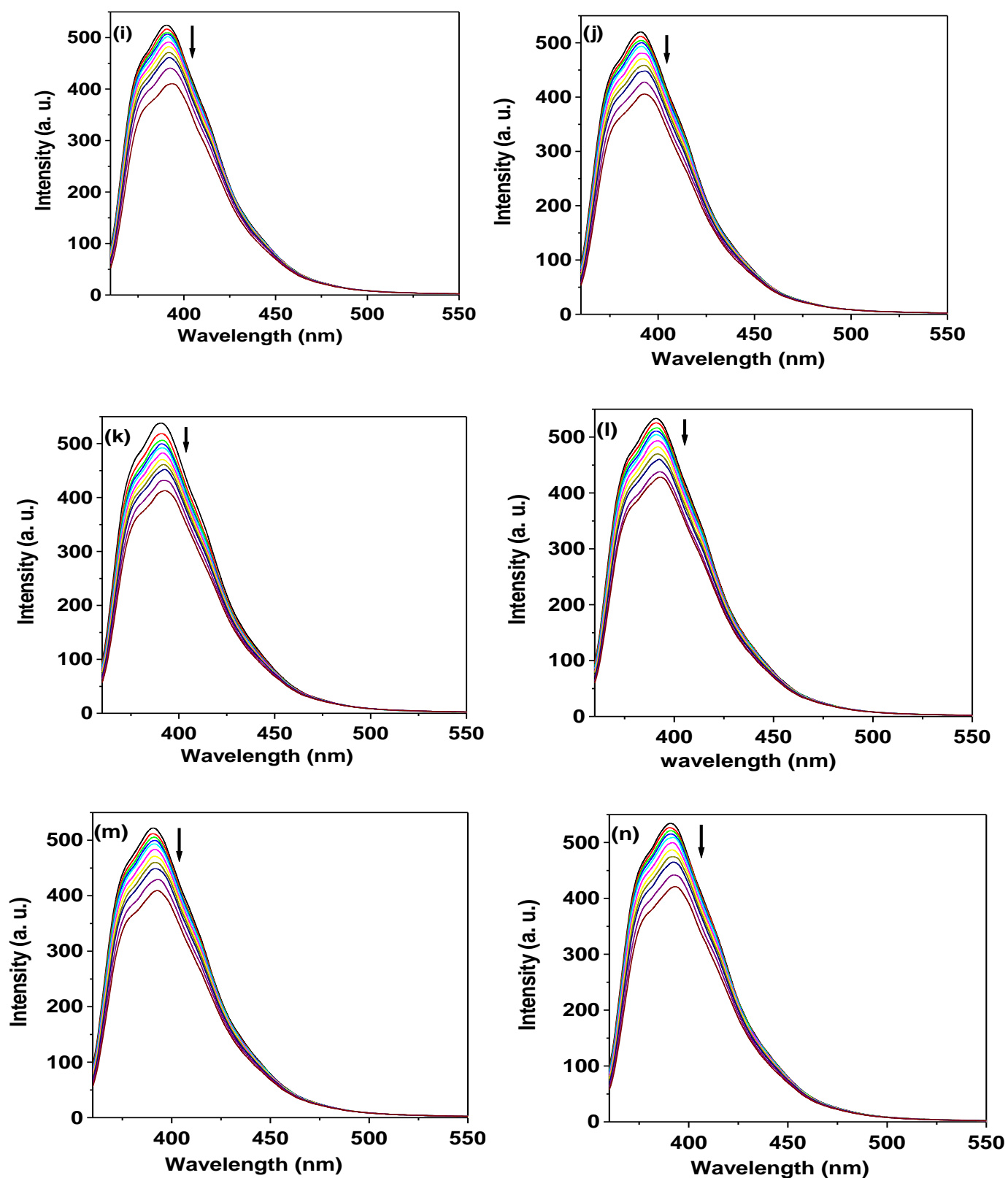


Figure S11: Fluorescence titration spectra of receptor (20 μM in CH₃CN/ H₂O, 40/60, v/v, HEPES buffer solution) with (0- 10 equiv.) of (a) Zn²⁺, (b) Hg²⁺, (c) Cd²⁺, (d) Fe²⁺,

(e) Co^{2+} , (f) Ni^{2+} , (g) Pb^{2+} , (h) Cu^{2+} , (i) Mn^{2+} , (j) Ba^{2+} , (k) Ca^{2+} , (l) K^+ , (m) Mg^{2+} , (n) Na^+ respectively.

7. UV-vis titration spectra of the sensor with Fe^{3+} , Al^{3+} and Cr^{3+} :

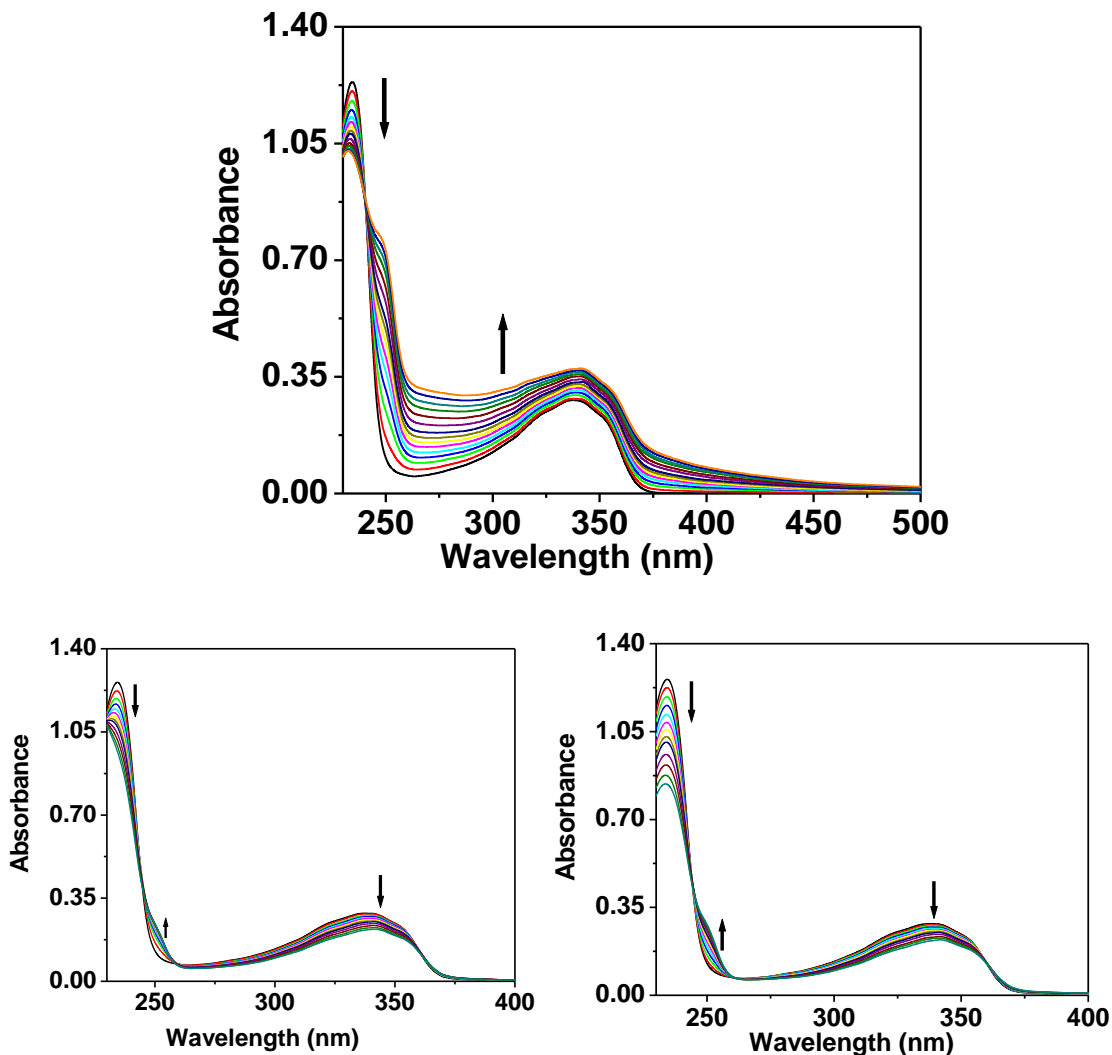


Figure S12: UV-vis titration spectra of NAQ with (a) Fe^{3+} , (b) Al^{3+} and (c) Cr^{3+} (0 to 10 equivalents) in $\text{CH}_3\text{CN} / \text{H}_2\text{O}$ (40/ 60, v/v, pH=7.4) solutions.

9. Crystallographic data and details of the structure determination of receptor (NAQ):

The data were collected using a Bruker-APEX II SMART CCD diffractometer with the graphite monochromated Mo- $\text{K}\alpha$ radiation ($\lambda = 0.71073$) at a detector distance of 5 cm and with APEX2 software. For data processing and absorption correction the packages SAINT¹ and SADABS² were used. The structures were solved by direct and Fourier methods and refined by full-matrix least squares based on F2 using SHELXTL³ and SHELXL-97⁴ packages. The crystallographic data and hydrogen bond geometry are

presented in Tables 1 and 2, respectively. Crystallographic data for receptor **NAQ** has been deposited with the Cambridge Crystallographic Data Center No. CCDC 888916.

Table 1:

CCDC No.	888916
Empirical Formula	C ₂₃ H ₁₅ N ₃ O ₄
Formula weight	397.38
Crystal system	
Space group	P b c a
T [K]	296 K
<i>a</i> [Å]	15.1430(4)
<i>b</i> [Å]	13.8141(4)
<i>c</i> [Å]	17.0179(5)
α [deg]	90
β [deg]	90
γ [deg]	90
Z	8
<i>V</i> [Å ³]	3559.92(17)
<i>D</i> _{calc} [g/cm ³]	1.483
<i>F</i> [000]	1648.0
Crystal size [mm]	0.10 x 0.20 x 0.30
Theta min-max [deg]	2.3, 27.1
μ [mm ⁻¹]	0.104
Reflections collected	34767
Unique reflections	3918
Observed reflections	2982
<i>R</i> [$F^2 > 2\sigma(F^2)$]	0.0394
w <i>R</i> (F^2)	0.1561

References:

- (1) APEX-II, SAINT-Plus, and TWINABS; Bruker-Nonius AXS, Inc.: Madison, WI, 2004
- (2) Sheldrick, G. M. SAINT, version 6.02 and SADABS, version 2.03; Bruker AXS, Inc.: Madison, WI, 2002.
- (3) SHELXTL, version 6.10; Bruker AXS, Inc.: Madison, WI, 2002.
- (4) Sheldrick, G. M. SHELXL-97, Crystal Structure Refinement Program; University of Göttingen: Germany, 1997.